802 MHz ERL Cavity Design and Development*

F. Marhauser#, S. Castagnola, W.A. Clemens, J. Dail, P. Dhakal, J. Henry,
F. Fors, R.A. Rimmer, L. Turlington, R.S. Williams, Jefferson Laboratory, Newport News, USA
R. Calaga, E. Jensen, K-M. Schirm, CERN, Geneva, Switzerland

Abstract

Two niobium and three copper prototype cavities resonating at 802 MHz were built at JLab in the frame of a collaboration with CERN for ongoing LHeC [1] and FCC initiatives [2]. This document describes the cavity design concept, fabrication efforts and high power RF test results for the two niobium cavities.

INTRODUCTION

Following a general memorandum of understanding signed between the European Organization for Nuclear Research (CERN) and Jefferson Laboratory (JLab) to cooperate in the development of superconducting radio frequency (SRF) accelerator technologies for a Future Circular Collider (FCC) hosted by CERN, an agreement for a joint work statement (JWS) has been established. The JWS aimed to develop a conceptual design, fabricate, chemical post-process, and vertical test one five-cell and one single-cell elliptical SRF cavity resonating at 802 MHz. This supports R&D efforts for both the Large Hadron electron Collider (LHeC) and the electron-hadron collider as part of the FCC studies (FCC-he). Both machines conceive utilizing five-cell 802 MHz SRF cavities in a 60 GeV three-pass racetrack Energy Recovery Linac (ERL) for a linac-ring hadron-electron collider configuration. Note that five-cell 802 MHz SRF cavities are also envisioned for the lepton-lepton collider (FCC-ee) in the last RF staging scenario for the ttbar physics program [3].

The aim of the Nb prototype development was to validate the basic RF cavity design in a high power vertical test setup at 2 K helium bath temperature. The exact RF operating frequency is 801.58 MHz, i.e. the 20th harmonic of the colliding bunch repetition frequency. This frequency choice is in synergy with RF system developments at CERN and keeps beam-beam interactions small.

The project started officially in July 2016, when funding became available. Though the focus of the project was on the Nb cavity development, JLab also made OFHC copper cavities to support ongoing Nb thin-film coating R&D at CERN. In addition, an OFHC copper cavity was built for low power bench measurements, for which multiple half-cells can be mechanically clamped together. Presently, a mock-up can be created with up to two full cells, but more cells can be added later if desired. Figure 1 depicts all cavities fabricated. The list below summarizes the manufacturing efforts in chronological order.

Authored by Jefferson Science Associates, LLC under U.S. DOE Contract No. DE-AC05-06OR23177 with funding from the JWS 2015S009. The U.S. Government retains a non-exclusive, paid-up, irrevocable, world-wide license to publish or reproduce this manuscript for U.S. Government purposes.
marhause@jlab.org

- Single-cell fine grain, high-purity Nb cavity
- Five-cell fine grain, high-purity Nb cavity
- Two single-cell OFHC copper cavities
- One low power OFHC copper cavity with variable number of cells

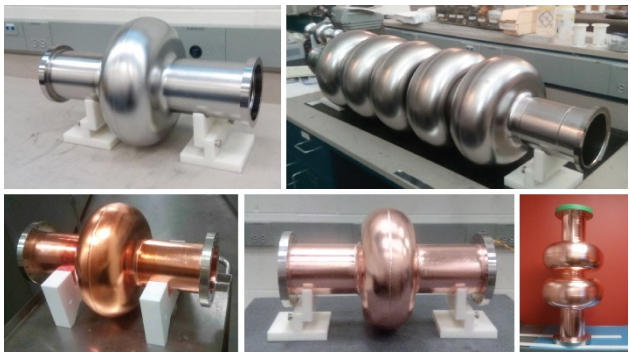

Figure 1: Ensemble of cavities fabricated for CERN.

CAVITY DESIGN

The main design goal was to optimize a five-cell SRF cavity suitable for an ERL at high beam currents. A single-cell cavity is simply made up of end half-cells attached to beam tubes. The design started from a 'blank sheet' aiming at balancing all key performance parameters considering RF, mechanical and beam-dynamical aspects. First, numerical RF calculations were carried out varying the cavities' inner (mid) half-cell shapes. This already provides crucial optimization parameters (e.g. E_{pk}/E_{acc}, B_{pk}/E_{acc}, and $R/Q{\cdot}G$) applicable for the five-cell cavity since the mid half-cells can be readily joined to obtain a cavity with any number of cells. The end half-cells attached to beam tubes were optimized separately. Performing the optimization studies on the mid half-cells allowed surveying a large number of different geometries within a reasonable time frame for a statistical optimization approach. Figure 2 for instance depicts the results for more than 1000 half-cell geometries resonating at 802 MHz. Herein, B_{pk}/E_{acc} and $R/Q{\cdot}G$ are plotted in dependence on E_{pk}/E_{acc}. In this example the iris diameter of the half-cell has been kept fixed so to allow a fair comparison of the different shapes. A general goal for an SRF cavity is to minimize both surface peak field enhancement ratios, B_{pk}/E_{acc} and E_{pk}/E_{acc}, simultaneously since it will theoretically shift the thermal breakdown limit and field emission onset to higher accelerating fields. The dashed curve is a hyperbolic fit encompassing the B_{pk}/E_{acc} vs. E_{pk}/E_{acc} data (orange dots) at the lower end. Consequently, it represents a threshold below which B_{pk}/E_{acc} cannot be lowered without increasing E_{pk}/E_{acc} and vice versa.

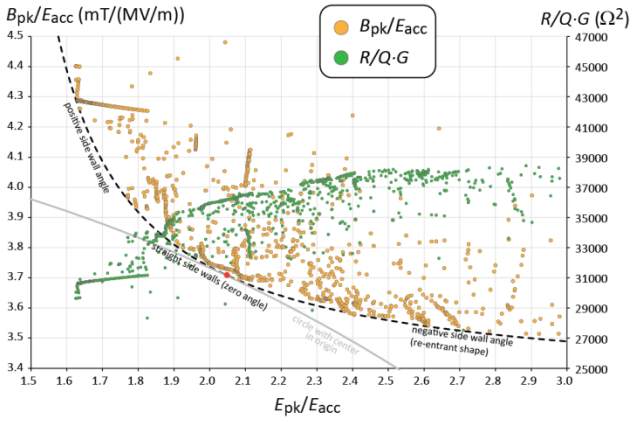

Figure 2: Numerical results for > 1000 half-cell structures at 802 MHz plotting B_{pk}/E_{acc} and $R/Q \cdot G$ in dependence on E_{pk}/E_{acc}, respectively (100 mm iris aperture).

When a cavity shape resides on the dashed line, the cell geometry can be deemed as optimized with respect to B_{pk}/E_{acc} and E_{pk}/E_{acc}. Figure 2 therefore graphically illustrates whether or not this is the case. Apparently, one may pick an optimized design from a whole branch of geometries by following the dashed curve. The final design should be selected with respect to the machine requirements. A cell shape is typically dubbed *High Gradient* when it yields a small E_{pk}/E_{acc}-value (relatively steep wall angles) and *Low Loss* for a small B_{pk}/E_{acc}-value (relatively shallow wall angles). The latter typically goes along with a high $R/Q \cdot G$-value (green dots), which is favourable to reduce the RF power losses into the helium bath according to:

$$P_{RF} = \frac{{V_{acc}}^2}{R/_{Q \cdot G}} \cdot R_s. \quad (1)$$

Herein V_{acc} is the accelerating voltage, R_S the average cavity surface resistance, R/Q the cavity characteristic shunt impedance, and G its geometry factor ($G = Q_0 \cdot R_s$ with Q_0 denoting the unloaded quality factor). Especially for machines operating in CW mode such as ERLs, the minimization of the dynamic losses is important to keep the costs for the helium refrigeration low. This affects both capital and operational expenditures. Given the scaling of the RF losses with V_{acc} squared, the optimum accelerating field in CW mode is typically ≤ 20 MV/m, which in turn mitigates issues with field emission a priori. Choosing a *Low Loss* shape is therefore favorable in such respect. Note however that a reduction of B_{pk}/E_{acc} - when moving along the dashed curve in Fig. 2 to the far right side - results in re-entrant structures (negative wall angle). While this does not impose concerns for normal-conducting cavities, it is practically not favorable for SRF cavities since chemical residues are harder to remove in the re-entrant area and are a performance risk factor.

To balance all critical RF performance parameters, we have selected a half-cell shape with straight side walls for prototyping. Such cell shapes actually reside in a regime, where the vector sum (Sqrt($(E_{pk}/E_{acc})^2$+ $(B_{pk}/E_{acc})^2$) is at or close to its overall minimum. The minimal value is illustrated by the intersection point (red) of the dashed curve with a circle (grey curve) having its center at the origin ($E_{pk}/E_{acc} = B_{pk}/E_{acc} = 0$). In this regime $R/Q \cdot G$ is still reasonably high before it would roll off for *High Gradient* structures.

As mentioned above, the iris aperture has been kept fixed in above example, yet it is a free optimization parameter. A smaller iris can shift both B_{pk}/E_{acc} and E_{pk}/E_{acc} to lower values, however it comes at the expense of the cavities' mechanical stiffness as well as a reduced cell-to-cell coupling (k_{cc}) of RF fields. This specifically impedes the Higher-Order-(HOM) Mode damping capability. By performing similar computations as shown in Fig. 2 for various iris apertures and applying the same optimization concept, an iris ID of 130 mm has been chosen eventually as a trade-off. Table 1 summarizes the relevant RF parameters of the five-cell cavity design. Specifically, k_{cc} is 3.2%, which is much larger than for the prominent TESLA cavity (1.89%), while B_{pk}/E_{acc} is even slightly smaller by design [4].

Table 1: RF Parameters of the Five-Cell Cavity

Parameter	**Unit**	**Value**
f_0 (cold, nominal)	MHz	801.58
L_{act}	mm	917.9
$R/Q = V_{acc}/(\omega \cdot W)$	Ω	523.9
G	Ω	274.6
E_{pk}/E_{acc}		2.26
B_{pk}/E_{acc}	mT/(MV/m)	4.2
Iris ID (= tube ID)	mm	130
k_{cc}	%	3.2

Note that for prototyping we have opted for a 'single deep-drawing die' design to minimize tooling costs. This is not a requirement for production cavities. Thus, end half-cells exhibit the same cell contour as mid-cells, but must be trimmed at the equator to provide a flat fundamental field profile for the accelerating mode as illustrated in Fig. 3.

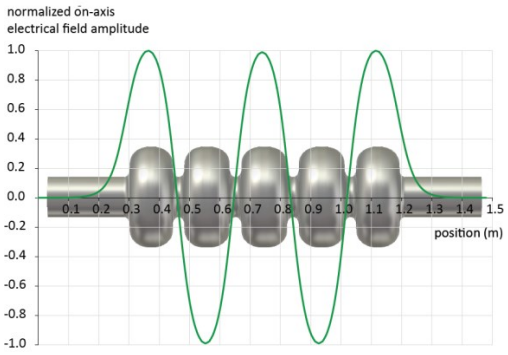

Figure 3: TM_{010} π-mode field profile as designed.

The cell equators therefore incorporate short flat sections so to avoid cutting into the elliptical portion of the end-cells after trimming. If at all necessary, each end cell could be geometrically (and independently) fine-tuned for

production cavities in order to selectively improve the damping of performance-limiting HOMs [5].

CAVITY PRODUCTION

For the Nb and Cu cavity fabrication we had to produce new or modify existing tools, respectively. For example, new tools included deep-drawing dies for half-cells, rolling dies for beam tubes, tuning plates, special beam tube adapters for the electropolishing (EP) machine, and support hardware for the vertical RF test cage for both the single-cell and five-cell cavity. All sub-assemblies of the Nb cavities were electron-beam-welded by overlapping partial penetration (butt) welds conducted from the outside and inside. This welding scheme was employed to avoid potential risks of blown-through holes at equators given previous experiences. However for the two welded Cu single-cell cavities, single-pass full penetration welds were conducted at the cell equators. No issues were experienced in either case. The Cu cavities were not further post-processed at JLab since they will be treated at CERN for Nb sputtering. Before testing the Nb cavities in JLab's vertical test area (VTA), the main post-processing steps listed in Table 2 have been carried out.

Table 2: Main Post-Processing Steps for the Nb Cavities

Parameter	Unit	1-Cell	5-Cell
Bulk BCP[a]	µm	160	216
High-T furnace bake	°C, hrs	800, 3	800, 3
Final EP[b]	µm	30	30
1st HPR cycles		2	4
Low-T bake-out	°C, hrs	120, 12	120, 12

BCP = buffered chemical polishing, HPR = High Pressure Water rinsing, [a] removal by in situ ultrasonic thickness gauge measurement at cell equator, [b] measured by integrated current method

RF TEST RESULTS

The latest RF vertical test results for both Nb cavities are summarized in Fig. 4 plotting the Q_0-values at 2 K temperature versus the accelerating field, E_{acc}. For the five-cell cavity a re-rinse has been conducted after the first test showed relatively strong field emission at the quench limit though the results were principally reproduced in the shown second test. Since for both cavities stainless steel blank flange test hardware was employed, it is important to subtract the artificial normal-conducting RF losses, which otherwise lead to a significant contribution to the effective surface resistance given the rather high Q_0-values of the cavities. The measurement results for both cavities well overlap at low fields yielding $Q_0 \sim$ 5e10 in maximum. The Q_0-offset visible at high fields could be due to trapped magnetic fluxes in the single-cell cavity after first quenching. Both cavities were eventually quench-limited with only minor field emission detectable. The five-cell cavity quenched at 30.1 MV/m (B_{pk} = 126 mT), while the single-cell cavity quenched at 32.3 MV/m (B_{pk} = 129 mT). In both cases a soft multipacting barrier (MP) starting around 10 MV/m had been observed that could be easily processed. For the single-cell cavity this however led to sparse data (greyed-out) in the MP regime. No further RF conditioning in the MP barrier was invested at the time due to schedule constraints allowing other VTA tests to proceed. Yet, the single-cell cavity is scheduled for a re-rinse and a re-test to produce 'clean' results. A measurement of the residual resistance based on temperature-dependent Q_0-values for the single-cell cavity at low field yielded 3.19 ± 0.79 nΩ for the Nb sheets employed.

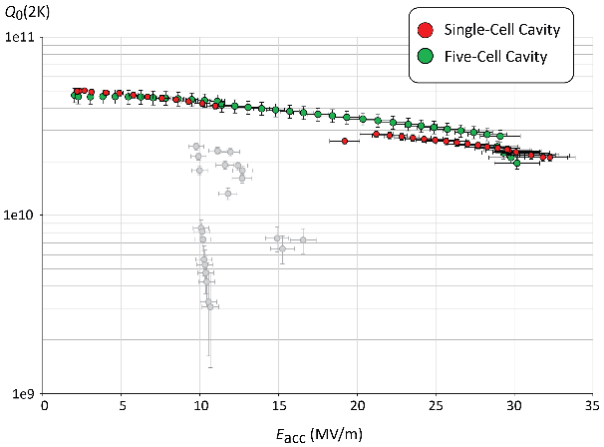

Figure 4: Combined VTA results for the five-cell and single-cell cavity as measured at 2 Kelvin.

CONCLUSION

A small series fabrication of 802 MHz Nb and Cu cavities dedicated for CERN's FCC and LHeC initiatives has been completed at JLab. Both Nb cavities achieved very high Q_0-values applying only standard post-processing methods. Given the low BCS resistance at 802 MHz, N-doping or N-infusion techniques might not result in significantly higher Q_0-values, though some R&D will proceed with the single-cell cavity. With a Q_0 of 3e10 up to ~27 MV/m the five-cell cavity exceeds present operational specifications for both the LHeC and FCC-eh machines ($Q_0 \leq$ 2e10, $E_{acc} \leq$ 20 MV/m). The cavity design has been meanwhile adopted for the Powerful ERL for Experiments (PERLE) facility at Orsay/France [6], which is proposed as a testbed to demonstrate LHeC and FCC-he principles.

REFERENCES

[1] LHeC Study Group, "A Large Hadron Electron Collider at CERN", Sept. 2012, ***arXiv:1206.2913v2***

[2] http://cern.ch/fcc

[3] M. Boscolo, "FCC-ee machine design overview", FCC week 2018, Amsterdam, Netherlands, 9. April 2018.

[4] B. Aune et al., "The Superconducting TESLA cavities", Phys. Rev. ST Accel. Beams 3, 092001, March 2000, ***arXiv:physics/0003011***

[5] F. Marhauser, "Next generation HOM-damping", Supercond. Sci. Technol. 30, 063002, May 2017, ***doi.org/10.1088/1361-6668/aa6b8d***

[6] PERLE: Powerful Energy Recovery Linac for Experiments - Conceptual Design Report, May 2017, ***arXiv:1705.08783***